



Contents lists available at ScienceDirect

## Journal of Materials Science &amp; Technology

journal homepage: [www.jmst.org](http://www.jmst.org)

# Preparation of $Ti_2AlC$ MAX Phase Coating by DC Magnetron Sputtering Deposition and Vacuum Heat Treatment



Zongjian Feng, Peiling Ke\*, Aiyang Wang\*

Key Laboratory of Marine Materials and Related Technologies, Zhejiang Key Laboratory of Marine Materials and Protective Technologies, Ningbo Institute of Materials Technology and Engineering, Chinese Academy of Sciences, Ningbo 315201, China

## ARTICLE INFO

## Article history:

Received 11 November 2014

Received in revised form

8 December 2014

Accepted 26 December 2014

Available online 30 October 2015

## Key words:

 $Ti_2AlC$ 

MAX phase

Coating

Magnetron sputtering

Microstructure

Due to the excellent corrosion resistance and high irradiation damage resistance,  $Ti_2AlC$  MAX phase is considered as a candidate for applications as corrosion resistant and irradiation resistant protective coating. MAX phase coatings can be fabricated through firstly depositing a coating containing the three elements  $M$ ,  $A$ , and  $X$  close to stoichiometry of the MAX phases using physical vapor deposition, followed by heat treatment in vacuum. In this work,  $Ti-Al-C$  coating was prepared on austenitic stainless steels by reactive DC magnetron sputtering with a compound  $Ti_{50}Al_{50}$  target, and  $CH_4$  used as the reactive gas. It was found that the as-deposited coating is mainly composed of  $Ti_3AlC$  antiperovskite phase with supersaturated solid solution of Al. Additionally, the ratio of  $Ti/Al$  remained the same as that of the target composition. Nevertheless, a thicker thermally grown  $Ti_2AlC$  MAX phase coating was obtained after being annealed at  $800\text{ }^\circ\text{C}$  in vacuum for 1 h. Meanwhile, the ratio of  $Ti/Al$  became close to stoichiometry of  $Ti_2AlC$  MAX phases. It can be understood that owing to the higher activity of Al, it diffused quickly into the substrate during annealing, and then more stable  $Ti_2AlC$  MAX phases transformed from the  $Ti_3AlC$  antiperovskite phase.

Copyright © 2015, The editorial office of Journal of Materials Science & Technology. Published by Elsevier Limited. All rights reserved.

## 1. Introduction

MAX phases are a family of the layered compounds with a general formula  $M_{n+1}AX_n$  ( $n = 1, 2, \text{ or } 3$ ), where  $M$  is a transition metal,  $A$  is an A-group element, and  $X$  is either C or N<sup>[1]</sup>. MAX phases possess unique properties combining that of ceramics and metals, such as high electrical and thermal conductivity, good machinability, excellent thermal shock resistance and damage tolerance, high elastic modules, high temperature strength, and both superior oxidation and corrosion resistances etc.<sup>[2,3]</sup>. Moreover, quite recently, MAX phases have also been found to be irradiation tolerant<sup>[4]</sup>.

Obviously, the coating approach can result in substantial cost reduction and can fully take advantage of the property of both MAX phases and substrate materials to improve the structural and chemical stabilities of the substrate materials under severe conditions, such as high temperature, high corrosion as well as high irradiation. Thus, physical vapor deposition (PVD), such as magnetron sputtering<sup>[5–8]</sup>, high-power impulse magnetron sputtering<sup>[9,10]</sup> and cathodic arc deposition<sup>[11,12]</sup>, has been developed to prepare MAX

phases coatings. However, because MAX phases belong to a complex hexagonal structure with long  $c$ -axis, problem with high deposition temperature, phase purity and process control are likely causes for the limited application of MAX phase coatings. Recently, a dense and thicker thermally grown MAX phase coating can be obtained by using a preferred method, in which a coating containing the three elements  $M$ ,  $A$ , and  $X$  was firstly deposited in appropriate composition using PVD, followed by heat treatment in vacuum<sup>[13–16]</sup>. One of the most important factors to obtain pure MAX phase coating using this method is the composition of as-deposited coating which should be close to stoichiometry of the MAX phases. Generally, two different ways have been applied for this purpose. One is to deposit the coating from MAX phase compound target. This would significantly increase the cost of coating preparation. The other way is to co-deposit from elemental targets; unfortunately, this would make the coating deposition process control more complicated and difficult.

Meanwhile, magnetron sputtering from only one compound target would simplify the deposition process and enable upscaling. Thus, in this work,  $Ti_2AlC$  MAX phase coating is prepared on austenitic stainless steels through the reactive DC magnetron sputtering deposition with a compound  $TiAl$  target and methane as the reactive gas in the unintentional heating condition, and then followed by annealing in vacuum. The phase formation and microstructure evolution of the as-deposited  $Ti-Al-C$  coating after annealing was investigated.

\* Corresponding authors. Prof., Ph.D.; Tel.: +86 574 86685170; Fax: +86 574 86685159.

E-mail addresses: [kepl@nimte.ac.cn](mailto:kepl@nimte.ac.cn) (P. Ke), [aywang@nimte.ac.cn](mailto:aywang@nimte.ac.cn) (A. Wang).

## 2. Experimental

Type 316L austenitic stainless steels (316LSS) were used as the substrates alloy for the present work. The nominal composition of 316LSS is given as follows: Fe, bal; Cr, 16.0–18.0; Ni, 10.0–14.0; Mo, 2.0–3.0; C  $\leq$  0.03; Mn  $\leq$  2.00; Si  $\leq$  1.00; P  $\leq$  0.045; S  $\leq$  0.03. The steel plates were cut into specimens with the size of 15 mm  $\times$  10 mm  $\times$  2 mm, followed by grinding with 1000-grit SiC paper and degreasing with acetone. Then, the samples were loaded into the DC magnetron sputtering deposition system to deposit Ti–Al–C coating.

Prior to deposition, the chamber was evacuated to a pressure of approximately  $4.6 \times 10^{-3}$  Pa. Depositions were performed with compound  $\text{Ti}_{50}\text{Al}_{50}$  (at.%) target (400 mm  $\times$  100 mm  $\times$  10 mm) in an Ar/CH<sub>4</sub> atmosphere with CH<sub>4</sub> as the reactive gas. During the deposition process, the applied power on the  $\text{Ti}_{50}\text{Al}_{50}$  target was kept at about 1.6 kW. The substrate bias voltage was kept at  $-250$  V, and no intentional heating of the substrates was conducted. The specimens constantly rotated during the coating process. The coating thickness was controlled by adjusting deposition time. Unless mentioned, the deposition time in the present work was 10 h. Annealing treatment of the as-deposited coating was conducted at 800 °C in vacuum for 1 h to the formation of the  $\text{Ti}_2\text{AlC}$  MAX phase. Before the annealing process, the chamber was pumped down to  $1.0 \times 10^{-2}$  Pa and heated to the annealing temperature at a heating rate of about 10 °C/min.

X-ray diffraction (XRD) was conducted to analyze the phase structure of coatings using a Bruker D8 diffractometer with  $\text{CuK}\alpha$  radiation source. Raman spectra were collected at room temperature in a Renishaw InVia-reflex Raman spectrometer. A scanning electron microscope (SEM) of FEI Inspect FSEM equipped with an Oxford energy dispersive X-ray (EDX) microanalysis system was used for imaging and microanalysis.

## 3. Results and Discussion

Fig. 1 shows the XRD patterns of the as-deposited and the annealed Ti–Al–C coatings on 316LSS for different deposited times. The crystalline structure of the as-deposited Ti–Al–C coating is unaffected by the deposition time. All the as-deposited Ti–Al–C coatings for different deposited times are mainly composed of  $\text{Ti}_3\text{AlC}$  antiperovskite phase. With increasing the deposition time, the thickness of the as-deposited coating increased. Nevertheless, the thickness of the as-deposited coatings plays an important role in the phase formation of the annealed coating. In the case of coatings deposited for 6 h, the following annealed Ti–Al–C coating is composed of  $\text{Ti}_2\text{AlC}$ ,  $\text{Ti}_3\text{AlC}$  and TiC, while in the case of coatings deposited for 8 h and 10 h, they are mainly composed of  $\text{Ti}_2\text{AlC}$  with small amount of  $\text{Ti}_3\text{AlC}$ . It is clear that the  $\text{Ti}_2\text{AlC}$  MAX phase can be formed by annealing at 800 °C in vacuum for 1 h. Moreover, it could be deduced that a minimum coating thickness was required to obtain high purity  $\text{Ti}_2\text{AlC}$  coating as mass transfer may occur during high temperature annealing. Once the thickness of the as-deposited coating exceeded the critical value, the interdiffusion between coating and substrate during annealing at high temperature would cause the composition of the coating to fall into a region which favors the formation of the  $\text{Ti}_2\text{AlC}$  phase.

To confirm the  $\text{Ti}_2\text{AlC}$  phase formation in the annealed Ti–Al–C coating, Raman spectroscopy was also used in this study. The spectra of the annealed Ti–Al–C coating in Fig. 2 show two peaks at  $\omega_2 \sim 269 \text{ cm}^{-1}$  and  $\omega_4 \sim 359 \text{ cm}^{-1}$  corresponding to the first-order vibration peaks of  $\text{Ti}_2\text{AlC}$ , which is consistent with previous literature<sup>[17]</sup>. The peak  $\omega_1$  (usually at  $\sim 150 \text{ cm}^{-1}$ ) in the Raman spectra of the  $\text{Ti}_2\text{AlC}$  cannot be distinguished from backgrounds in

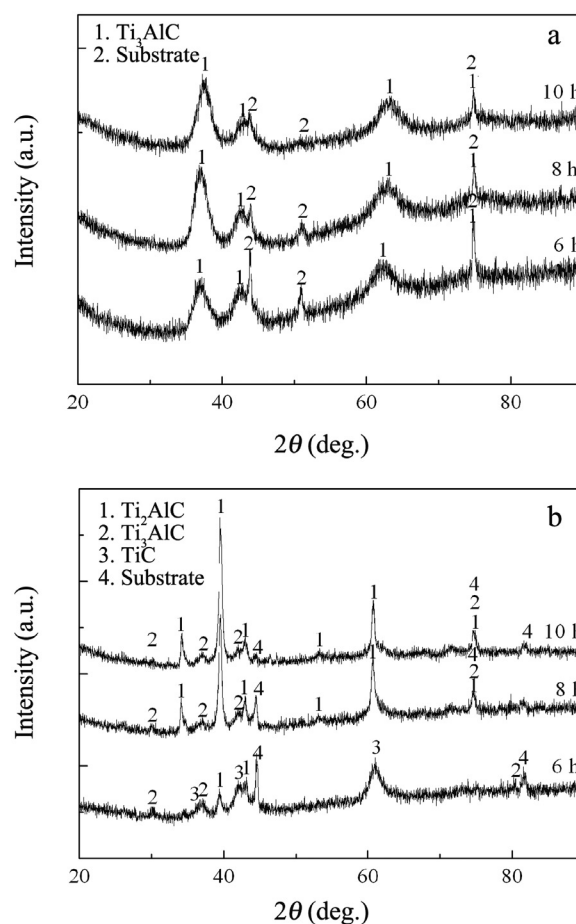


Fig. 1. XRD patterns of the as-deposited (a) and the annealed (b) Ti–Al–C coatings on 316LSS for different deposited times.

this study. Therefore, taking the XRD results into account, it was clearly confirmed that the  $\text{Ti}_2\text{AlC}$  phase existed in the annealed Ti–Al–C coatings.

The surface and cross-sectional morphologies of the as-deposited Ti–Al–C coatings show uniform and crack free microstructure with a thickness of around 13  $\mu\text{m}$  (Fig. 3). The EDX results from the cross-sectional morphologies of the as-deposited coating are listed in Table 1. Because EDX cannot be used to accurately determine light elements, C and O are not shown. The ratio

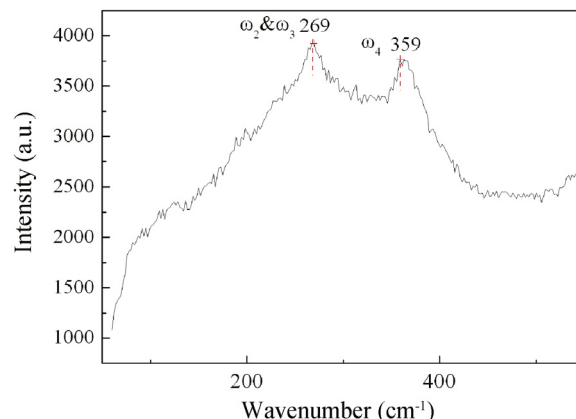
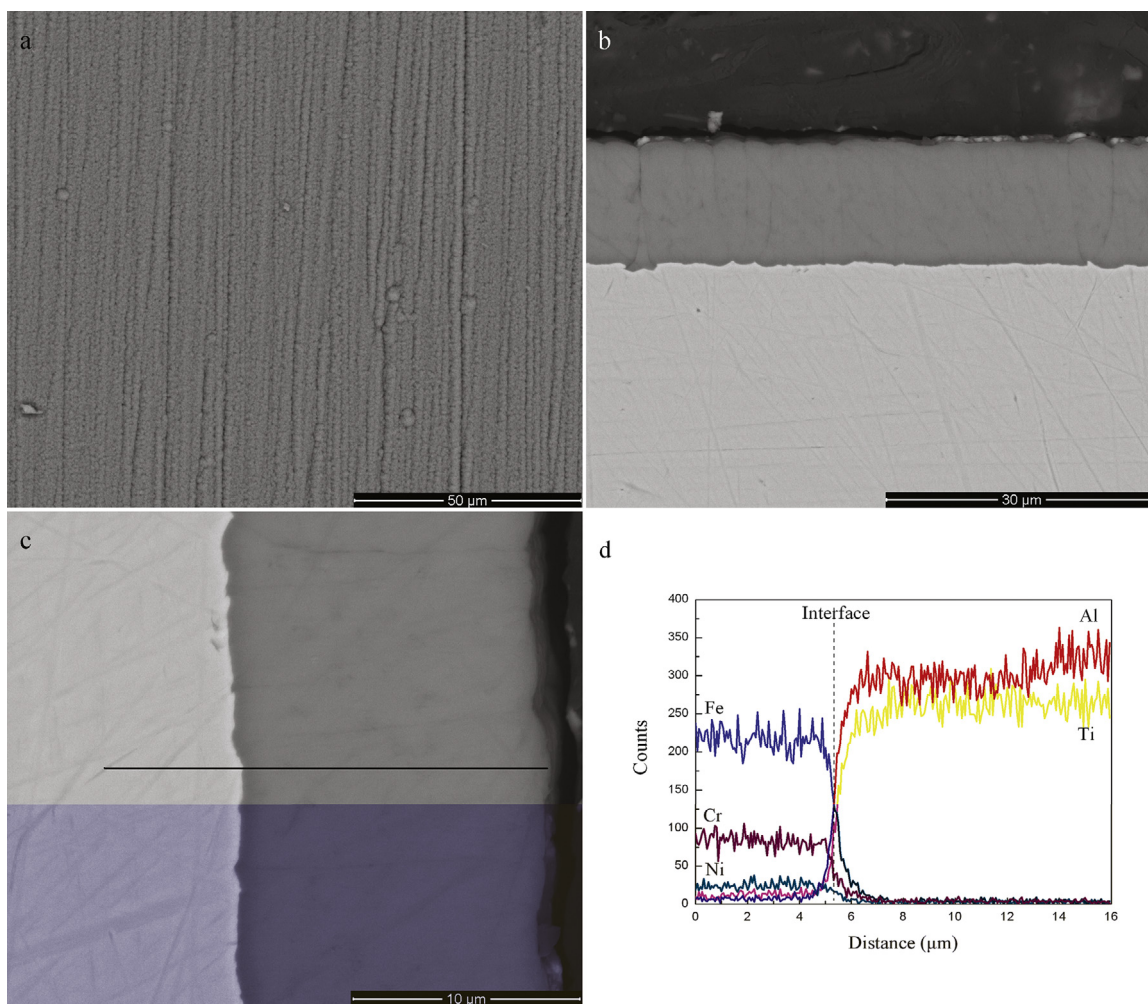


Fig. 2. Raman spectra of the annealed Ti–Al–C coatings.



**Fig. 3.** Surface morphology (a) and general view (b) of cross-sectional morphologies, and amplified view (c) of (b) of the as-deposited Ti–Al–C coatings; (d) the corresponding EDX line scan along the black line in (c).

of Ti/Al within the as-deposited coating almost remained the same as that of the target composition, and small amounts of Fe and Cr from the target holder also could be found in the as-deposited coating. However, neither diffraction peak of Al nor broadening phenomena of X-ray peak standing for amorphous could be observed in XRD patterns (Fig. 1(a)). It is reasonable to believe that Al is a supersaturated solid solution in  $\text{Ti}_3\text{AlC}$  antiperovskite phase in the as-deposited coating. Furthermore, Fig. 3(d) shows the corresponding EDX line scan along the black line in Fig. 3(c). The sharp composition change at the coating/substrate interface indicates that no interdiffusion occurred between the coating and the substrate during deposition.

Although some small cracks were observed in the surface morphology of the annealed Ti–Al–C coatings (Fig. 4(a)), the appearance of the original coating was retained to a certain extent. Formation of cracks in the annealed Ti–Al–C coating is attributed to the

mismatch of thermal expansion coefficient between  $\text{Ti}_2\text{AlC}$  ( $8.2 \times 10^{-6} \text{ }^\circ\text{C}^{-1}$ [18]) and 316LSS ( $21.9 \times 10^{-6} \text{ }^\circ\text{C}^{-1}$ [19]). Fig. 4(b, c) shows the cross-sectional morphologies of the annealed Ti–Al–C coating. The annealed Ti–Al–C coating is compact, but cracks were observed partly across the coating. However, the coating still shows a good adhesion to the substrate. The ratio of Ti/Al in the cross-sectional morphologies of the annealed coating is close to stoichiometry of  $\text{Ti}_2\text{AlC}$  phases (Table 1), which is higher than that in the as-deposited coating, suggesting that a large amount of Al has migrated from the coating into the substrate. Meanwhile, an Al-rich diffusion layer is also observed at the coating/substrate interface. The corresponding EDX line scan along the black line in Fig. 4(c) is shown in Fig. 4(d). The ratio of Ti/Al within the annealed coating tends to decrease slightly with the decrease in the distance to the coating/substrate interface. The Al content shows an abnormal tendency, as a valley formed at the coating/substrate interface, while the Al content in the substrate close to the coating/substrate interface is higher than the coating. The diffusion of other elements such as Ti, Fe, Cr and Ni follows concentration gradient. The following factors could account for this phenomenon. As Al is a supersaturated solid solution in  $\text{Ti}_3\text{AlC}$  antiperovskite phase in the as-deposited coating, Al possesses higher activity than Ti during high temperature annealing. So, the inward diffusion rate of Al is much higher than Ti. Moreover, owing to the fact that Al has a high affinity for substrate elements such as Fe, Cr and Ni, the rapid

**Table 1**  
Chemical composition of the as-deposited and annealed coating by EDX (in at.%)

Element	As-deposited	Annealed
Ti	52.92	62.65
Al	46.06	33.25
Fe	0.77	3.74
Cr	0.25	0.36

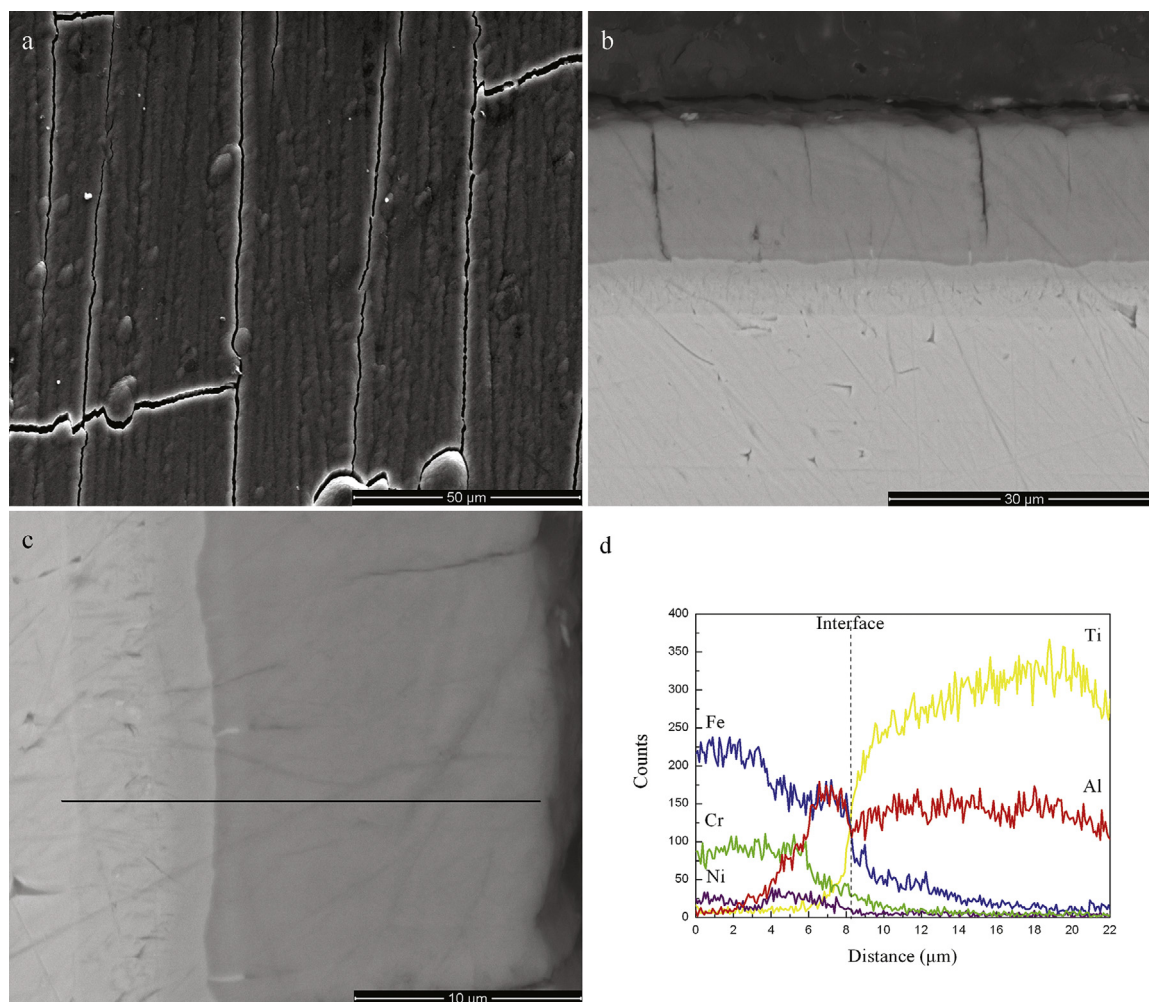


**Fig. 4.** Surface morphology (a) and general view (b) of cross-sectional morphologies and amplified view (c) of (b) of the annealed Ti–Al–C coatings; (d) the corresponding EDX line scan along the black line in (c).

formation of intermetallic compound in the substrate close to the coating/substrate interface resulted in depletion of Al at the coating/substrate interface and the uphill diffusion of Al from interface to Al-rich layer. Moreover, it is possible that Al diffused to the surface of the coating. However, Al-rich region were not observed on the surface of the coating. So Al may vaporize into the environment during annealing.

There are no  $Ti_2AlC$  phases in the as-deposited Ti–Al–C coating, due to the low ion energy of reactive DC magnetron sputtering deposition without intentional heating of the substrate. The ratio of Ti/Al is deviated far from the stoichiometry of  $Ti_2AlC$  phases. However, it is usually believed that the homogeneous mixture of Ti, Al and C at atomic level in the Ti–Al–C coating formed during reactive DC magnetron sputtering. During high temperature annealing, the excessive Al in the as-deposited coating quickly diffused into the substrate, and thus the ratio of Ti/Al became close to the stoichiometry of  $Ti_2AlC$  phases. Meanwhile,  $Ti_3AlC$  phase is not stable and prone to decomposition. In contrast,  $Ti_2AlC$  is the most stable phase in the Ti–Al–C system<sup>[20]</sup>. As a result, the reaction between  $Ti_3AlC$  phase and Al followed by nucleation and growth of  $Ti_2AlC$  phase becomes feasible. With the formation of  $Ti_2AlC$  phase and the destruction of the original coating structure, the remaining excessive Al would possess higher activity and continue to diffuse into the substrate, then further promote the formation of  $Ti_2AlC$  phase and finally high purity  $Ti_2AlC$  phase coating was achieved. In addition,

it is probable that Fe, Cr and Ni in the annealed coating are substitutional or interstitial solid solution in  $Ti_2AlC$  phase. Undoubtedly, the interdiffusion between the coating and the substrate alloy during high-temperature annealing plays an important role in the formation of high purity  $Ti_2AlC$  phase coating. Hence, the substrate effect should be considered for preparing  $Ti_2AlC$  phase coating by the DC magnetron sputtering deposition followed by annealing on different alloy substrates.

#### 4. Conclusion

To obtain  $Ti_2AlC$  phase coating, a Ti–Al–C coating was firstly deposited on the 316LSS by reactive DC magnetron sputtering with a compound  $Ti_{50}Al_{50}$  (at.%) with  $CH_4$  used as the reactive gas, followed by vacuum annealing treatment at 800 °C. The as-deposited coating was mainly composed of  $Ti_3AlC$  antiperovskite phase with supersaturated solid solution of Al, and the ratio of Ti/Al was also deviated far from the stoichiometry of  $Ti_2AlC$  phases. However, the annealing treatment gave rise to the successful formation of  $Ti_2AlC$  MAX phase coatings, and the ratio of Ti/Al became closer to the stoichiometry of  $Ti_2AlC$  MAX phases. The effect of interdiffusion between the coating and the alloy substrate during high-temperature annealing on the formation of high purity  $Ti_2AlC$  phase coating could not be neglected.

## Acknowledgments

This project is supported by the National Natural Science Foundation of China (Grant No. 51522106 and Grant No. 51401229), the National Science and Technology Major Project of China (Grant No. 2015ZX06004-001) and the Ningbo Municipal Natural Science Foundation (Grant No. 2014A610013).

## References

- [1] M.W. Barsoum, *Prog. Solid State Chem.* 28 (2000) 201–281.
- [2] P. Eklund, M. Beckers, U. Jansson, H. Högberg, L. Hultman, *Thin Solid Films* 518 (2010) 1851–1878.
- [3] Z.M. Sun, *Int. Mater. Rev.* 56 (2011) 143–166.
- [4] E.N. Hoffman, D.W. Vinson, R.L. Sindelar, D.J. Tallman, G. Kohse, M.W. Barsoum, *Nucl. Eng. Des.* 244 (2012) 17–24.
- [5] J.J. Li, L.F. Hu, F.Z. Li, M.S. Li, Y.C. Zhou, *Surf. Coat. Technol.* 204 (2010) 3838–3845.
- [6] J. Frodelius, P. Eklund, M. Beckers, P.O.Å. Persson, H. Högberg, L. Hultman, *Thin Solid Films* 518 (2010) 1621–1626.
- [7] J. Emmerlich, D. Music, J.M. Schneider, P. Eklund, O. Wilhelmsson, U. Jansson, H. Högberg, L. Hultman, *Acta Mater.* 55 (2007) 1479–1488.
- [8] V. Vishnyakov, J. Lu, P. Eklund, L. Hultman, J. Colligon, *Vacuum* 93 (2013) 56–59.
- [9] T.F. Zhang, Q.M. Wang, J. Lee, P.L. Ke, R. Nowak, K.H. Kim, *Surf. Coat. Technol.* 212 (2012) 199–206.
- [10] Y. Jiang, S. Mráz, J.M. Schneider, *Thin Solid Films* 537 (2013) 1–6.
- [11] J. Rosén, L. Ryves, P.O.Å. Persson, M.M.M. Bilek, *J. Appl. Phys.* 101 (2007) 056101.
- [12] M.C. Guenette, M.D. Tucker, M. Ionescu, M.M.M. Bilek, D.R. McKenzie, *Thin Solid Films* 519 (2010) 766–769.
- [13] W. Garkas, C. Leyens, A. Flores Renteria, *Adv. Mater. Res.* 89–91 (2010) 208–213.
- [14] J.J. Li, Y.H. Qian, D. Niu, M.M. Zhang, Z.M. Liu, M.S. Li, *Appl. Surf. Sci.* 263 (2012) 457–464.
- [15] Y. Yang, M. Keuneecke, C. Stein, L.J. Gao, J. Gong, X. Jiang, K. Bewilogua, C. Sun, *Surf. Coat. Technol.* 206 (2012) 2661–2666.
- [16] A. Abdulkadhim, T. Takahashi, D. Music, F. Munnik, J.M. Schneider, *Acta Mater.* 59 (2011) 6168–6175.
- [17] V. Presser, M. Naguib, L. Chaput, A. Togo, G. Hug, M.W. Barsoum, *J. Raman Spectrosc.* 43 (2012) 168–172.
- [18] M.W. Barsoum, M. Ali, T. El-Raghy, *Metall. Mater. Trans. A* 31 (2000) 1857–1865.
- [19] O. Sayman, F. Sen, E. Celik, Y. Arman, *Mater. Des.* 30 (2009) 770–774.
- [20] M.A. Pietzka, J.C. Schuster, *J. Phase Equilib.* 15 (1994) 392–400.